



Channel cracking in thin films on substrates of finite thickness

J.J. VLASSAK

Division of Engineering and Applied Sciences, Harvard University, Cambridge, MA 02138, U.S.A.

Abstract. Solutions are presented for the elastic plane-strain problem of a crack in a coating on a compliant substrate of finite thickness. Analysis of the problem shows that substrate thickness has a significant effect on the steady-state energy release rate for channel cracks. This is so over a wide range of elastic mismatch between film and substrate, but is especially important if the substrate is more compliant than the film. Relaxation of the film stress due to elastic deformation of the substrate also plays an important role. If the substrate is clamped around the edge, as would be the case for a coated membrane, the stress in the coating cannot relax and the energy release rate for channel cracking increases significantly with decreasing substrate thickness. If the film stress is allowed to relax, however, the driving force for cracking is reduced as the substrate thickness decreases. The results from this study are used to evaluate the change in curvature of a film/substrate assembly due to channel cracking, a quantity that is of interest for the experimental determination of stresses in thin films. An expression for the elastic extension of the substrate due to channel cracking is derived making it possible to evaluate the effect of cracking on the mechanical behavior of bilayer membranes. It is expected that the present study may lead to the development of new experimental techniques for measuring the fracture toughness of thin coatings.

Key words: Channel cracking, compliant substrate, thin film

1. Introduction

The last decade has seen enormous progress in the area of integrated circuits and micromachined devices. These engineering systems typically consist of thin films of dissimilar materials joined together on a substrate. As such, the films in these systems can be subjected to very high stresses, which may result in cracking or delamination of the films. Thus, the reliability of these systems often depends on the fracture behavior of the films comprising the device and a good understanding of the possible failure mechanisms makes it possible to design more reliable devices.

The current investigation is concerned with a failure mechanism that is often observed in thin films, i.e., the cracking of a coating on a compliant substrate. Figure 1 is a schematic representation of this problem. A film of thickness h_1 is bonded to a substrate of finite thickness h_2 . Both film and substrate materials are considered to be elastically isotropic with Young's moduli E_1 and E_2 , and Poisson's ratios ν_1 and ν_2 , respectively. The film is subjected to a stress $\sigma(y)$. A crack oriented perpendicular to the film surface and extending all the way to the film/substrate interface is introduced into the film. The goal of this investigation, then, is to derive the relevant fracture mechanics quantities describing this problem and to present these quantities in a fashion that is useful for the design of multilayered systems.

The technique used for solving the problem depicted in Figure 1 is based on the work by Gecit (1979), Lu and Erdogan (1983a, b), Civelek (1985), and Suo and Hutchinson (1989, 1990). Gecit (1979) solves a number of crack problems for surface layers bonded to elastic half spaces and presents some numerical results for select material combinations. Lu and

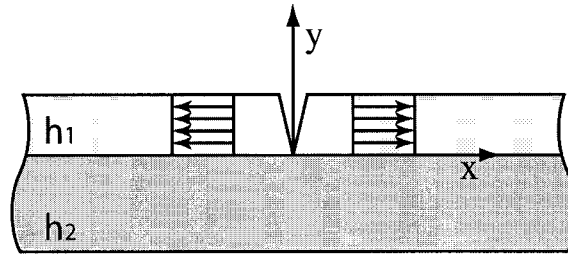


Figure 1. Schematic representation of a plane-strain crack in a film on a compliant substrate.

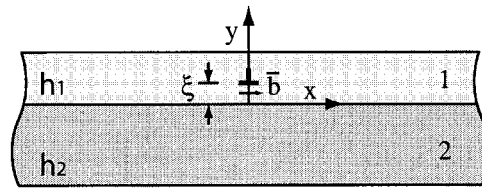
Erdogan (1983a, b) derive solutions for numerous crack problems in bilayer strips and present a detailed discussion of solution methods. They also provide the results of calculations for a limited materials set. Civelek (1985) discusses solution methods for problems involving infinite strips of a single material with arbitrarily arranged cracks, while Suo and Hutchinson (1989, 1990) address the problem of a crack lying at the interface or in the substrate of a bimaterial strip. Their method of solution consists of representing cracks by continuous distributions of dislocations. This solution technique was later applied by Beuth (1991) to study the case of a single crack in a coating on an infinite half space. He presents detailed results for a wide range of material combinations by formulating the results in terms of the two Dundurs (1969) parameters, α and β , of the materials system. Through use of the Dundurs parameters, it is possible to completely describe the materials dependence of a problem involving a body made of two isotropic, elastic materials with prescribed tractions. For plane-strain problems, α and β are given by

$$\alpha = \frac{\bar{E}_2 - \bar{E}_1}{\bar{E}_2 + \bar{E}_1}, \quad \beta = \frac{\mu_2(1 - 2\nu_1) - \mu_1(1 - 2\nu_2)}{2\mu_2(1 - \nu_1) + 2\mu_1(1 - \nu_2)}, \quad (1)$$

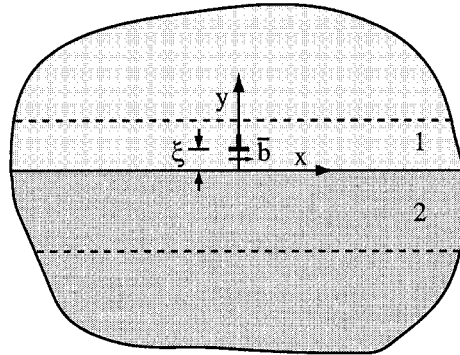
where $\bar{E} = E/(1 - \nu^2)$ and μ are the plane strain modulus and shear modulus, respectively. It is clear from Equation (1) that α can take values between -1 and 1 . For most practical material combinations, β varies from 0 to $\alpha/4$ (Suga et al., 1988).

The problem shown schematically in Figure 1 will be analyzed using the solution method described by Suo and Hutchinson (1989, 1990) and Hutchinson and Suo (1991). Numerical results will be presented for a wide range of material combinations through use of the Dundurs parameters of the bimaterial system as suggested by Beuth (1991). The results of this study are applicable to the case where coating and substrate are of comparable thickness, as well as to situations where the substrate is substantially thicker than the coating. Examples of the former may be encountered in MEMS devices with thin metal-coated polymer membranes that are electrostatically deflected or in devices with freestanding beams that consist of multiple layers. Examples where the substrate is much thicker than the coating can be found in many engineering applications. It is expected that the results of this investigation may be useful for measuring the fracture toughness of thin coatings by depositing the coating of interest onto a thin substrate and subsequently elastically deforming the coating/substrate system until channel cracks initiate at controlled defects and propagate in the film (Cook and Liniger, 1999).

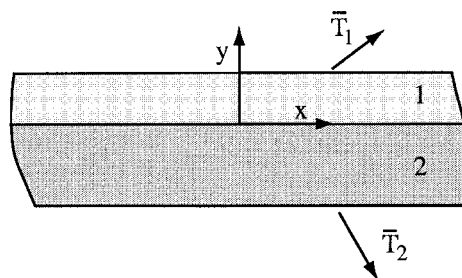
The present article is organized as follows. The analysis of the problem of interest is described in the next section. Since the solution technique has been formulated in detail by other authors (Suo and Hutchinson, 1989, 1990), only the steps particular to the problem at hand will be covered. The results from numerical calculations for a wide range of materials will be



(a)



(b)



(c)

Figure 2. Decomposition of the dislocation problem: (a) Edge dislocation in a bilayer strip. (b) Edge dislocation in an infinite bispace. (c) Bilayer strip with prescribed tractions.

presented in Section 3. Section 4 provides a discussion of how the results from Section 3 can be used in a number of practical applications.

2. Analysis

From a fracture mechanics point of view, the problem of a crack in a film with a tensile residual stress $\sigma(y)$ (Figure 1) is equivalent to that of a crack with a stress $-\sigma(y)$ applied

to its faces. This is the formulation that will be used to solve the problem. The crack in the coating is represented by a continuous distribution of edge dislocations. This approach leads to an integral equation in the dislocation density along the crack length with the normal stress due to one edge dislocation as kernel. Thus, the first step in the solution consists of determining the stress distribution around an edge dislocation in a bilayer strip. This stress distribution is readily derived if one realizes that the dislocation problem can be decomposed as illustrated in Figure 2. Figure 2a shows an edge dislocation with Burgers vector \mathbf{b} in a coating on a substrate of finite thickness. This problem can be described as the superposition of the problems depicted in Figures 2b and 2c. Figure 2b shows a dislocation in an infinite bimaterial. The dislocation causes tractions to arise on the planes that are indicated in the figure by means of the dashed lines and that correspond to the surfaces of the bilayer strip in the actual problem. Figure 2c shows a bilayer strip with tractions applied along its top and bottom boundaries, equal and opposite in sign to the tractions generated by the dislocation in the bimaterial. Superimposing the solution to this problem onto that for the problem depicted in Figure 2b results in the desired solution for a dislocation in a bilayer strip. The details of the derivation are presented in Appendix 1.

Once the stress distribution around an edge dislocation in a bimaterial strip is known, the crack can be modeled as a continuous distributions of edge dislocations with variable Burgers vector $b(\xi)$. The distribution of Burgers vectors $b(\xi)$ is determined from the condition that the normal stress on the crack faces equal $-\sigma(y)$. Integrating the stress component σ_{xx} of a dislocation with burgers vector $b(\xi)$ along $x = 0$, results in the following integral equation:

$$\begin{aligned} -\sigma(y) &= \int_0^{h_1} (\sigma_{xx}^d + \sigma_{xx}^s) b(\xi) d\xi \\ &= \frac{-\mu_1}{2\pi(1-\nu_1)} \int_0^{h_1} \left[\frac{1}{y-\xi} + F_d(0, y, \xi) + F_s(0, y, \xi) \right] b(\xi) d\xi. \end{aligned} \quad (2)$$

The first term in the integrand arises from the dislocation problem in Figure 2b and is integrated in the Cauchy principal value sense. The kernel functions $F_d(x, y, \xi)$ and $F_s(x, y, \xi)$ are derived from the solutions for the problems in Figures 2b and 2c, respectively. Because of the symmetry of the problem, the boundary condition for the shear stress on the crack surfaces is automatically satisfied.

The stress distribution at the tip of a crack in a uniform linear elastic material varies as one over the square root of the distance to the crack tip. If, however, the crack tip is located at the interface between two materials, as is the case in the present problem, the exponent, s , of the singularity is given by an equation derived by Zak and Williams (1963):

$$\cos s\pi + 2\frac{\alpha - \beta}{1 + \beta}(1 - s)^2 - \frac{\alpha + \beta^2}{1 - \beta^2} = 0. \quad (3)$$

Equation (2) is a singular integral equation that can be solved numerically using the collocation method. To that effect, the distribution of Burgers vectors $b(\xi)$ is expressed as a series of orthonormal polynomials, $L_k(t)$, with N unknown coefficients, C_k :

$$b(\xi) = \frac{1}{(1+t)^s} \sum_{k=0}^{N-1} C_k L_k(t), \quad (4)$$

where s is the stress singularity exponent given by Equation (3). Here, t is defined as

$$t = \frac{2\xi}{h_1} - 1 \quad -1 \leq t \leq 1, \tag{5}$$

and the $L_k(t)$ are polynomials of order k ($k = 0, 1, 2, \dots, N - 1$) that are mutually orthonormal with respect to the weight function

$$W(t) = \frac{1}{(1+t)^s} \tag{6}$$

in the interval $-1 \leq t \leq 1$. These polynomials can be calculated using a simple recurrence relation (Press et al., 1996). After substitution of Equation (4) into Equation (2), the integral equation is reduced to a set of linear equations in C_k . The unknown coefficients C_k are solved for by matching the traction boundary condition at N collocation points. Integrals are evaluated numerically using Gaussian quadrature with $W(t)$ as weight function, although some integrals require special treatment before they can be calculated accurately. A value of $N = 10$ was found to yield sufficiently accurate results. Once the function $b(\xi)$ is known, the components of the stress and displacement fields are readily calculated. The crack opening displacement, for instance, is given by

$$\delta(y) = \int_0^y b(\xi) \, d\xi. \tag{7}$$

3. Results and discussion

The procedure discussed in the previous section makes it possible to analyze channel cracking in coatings with arbitrary stress profiles through the thickness of the coatings. Consider a coating deposited onto a compliant substrate that is securely clamped around the edge. If the deposition stress is independent of film thickness, the residual stress in the coating, σ_{res} , is constant. When the substrate is released, however, the stresses in coating and substrate change due to the elastic deformation of the substrate. A straightforward analysis using plate bending theory leads to the following expression for the stress distribution in the film, $\sigma(y)$, after the substrate has been released:

$$\sigma(y) = \bar{\sigma} + \left(\frac{y}{h_1} - \frac{1}{2} \right) \Delta, \tag{8}$$

where

$$\frac{\bar{\sigma}}{\sigma_{\text{res}}} = \frac{1 + \Sigma\eta^3}{(\Sigma\eta^2 - 1)^2 + 4\Sigma\eta(\eta + 1)^2},$$

$$\frac{\Delta}{\sigma_{\text{res}}} = \frac{-6\eta^2(1 + \eta)\Sigma}{(\Sigma\eta^2 - 1)^2 + 4\Sigma\eta(\eta + 1)^2},$$

$$\Sigma = \frac{E_1}{1 - \nu_1} \bigg/ \frac{E_2}{1 - \nu_2} \quad \text{and} \quad \eta = h_1/h_2.$$

Thus, the stress takes on a linear distribution with $\bar{\sigma}$ the average stress in the coating and Δ/h_1 the slope of the distribution. Figure 3 depicts the stress in the film after the substrate is released. When the film thickness is small compared to that of the substrate, the film stress remains unchanged. As the substrate thickness decreases, the average stress in the coating drops

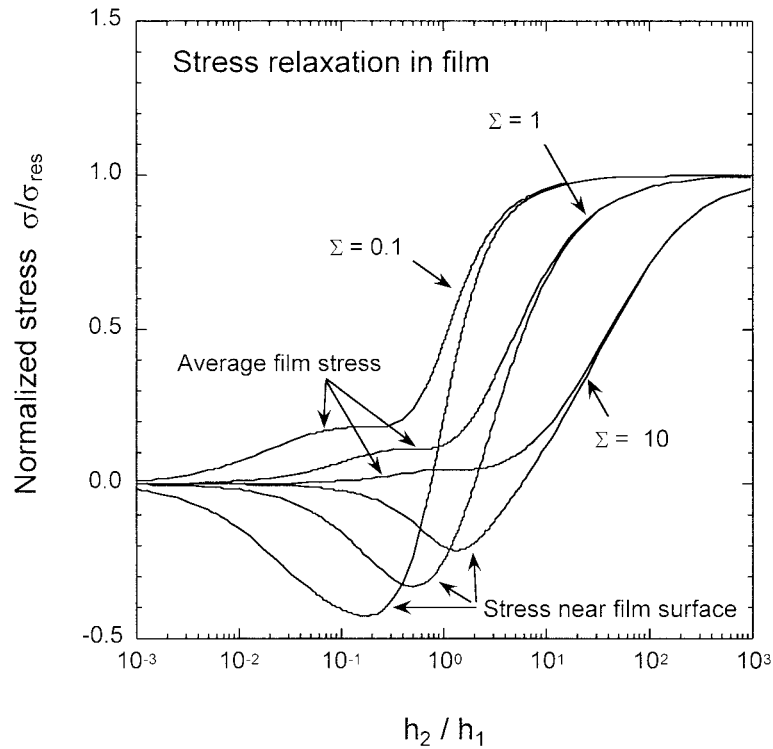


Figure 3. Average film stress and stress near the film surface after a film with initial residual stress σ_{res} has been allowed to relax by elastic deformation of the substrate.

off rapidly, reducing the driving force for channel cracking in the film. When the substrate thickness is comparable to that of the film, however, Δ goes through a pronounced minimum. As a result, the stress near the surface of the film, $(\bar{\sigma} + \Delta/2)$, changes sign. Thus, a film that is originally in compression, can go into tension when the substrate is released. This could result in the rather unexpected behavior where a film that is deposited in compression exhibits channel cracking.

Channel cracks have been analyzed for both constant and linear stress distributions in the film. In the following paragraphs, results will be presented separately for the case where the stress in the film is constant and equal to $\bar{\sigma}$, and for the case where the stress varies linearly from $-\Delta/2$ to $\Delta/2$. If the film/substrate assembly can be regarded as a thin plate or membrane clamped around its edge, the results for the constant stress distribution are applicable. Examples of this case can be found in the MEMS industry where thin membranes often serve as substrates for other coatings. If the substrate is released after the film deposition process, the stress distribution in the coating consists of both a constant and a linear term as described by Equation (8). In this case, the solution is found by superimposing the appropriate results for constant and linear stress distributions.

To analyze the crack problem illustrated in Figure 1, a generalized mode I stress intensity factor is defined as

$$K_I = \lim_{y \rightarrow 0^-} [(-2\pi y)^s \sigma_{xx}(0, y)]. \quad (9)$$

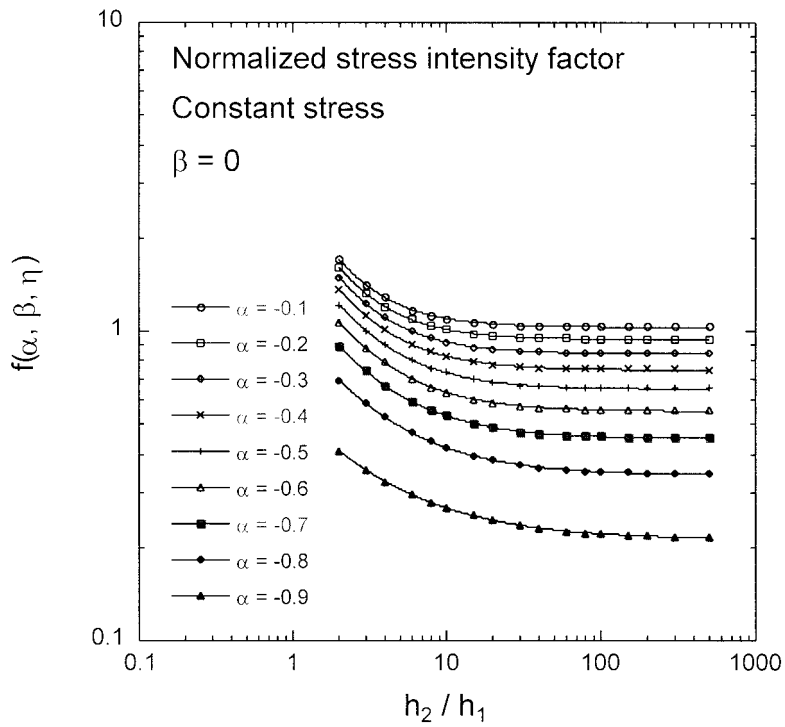


Figure 4. Normalized stress intensity factor as a function of substrate thickness for a film with a constant stress distribution. Substrate more compliant than film.

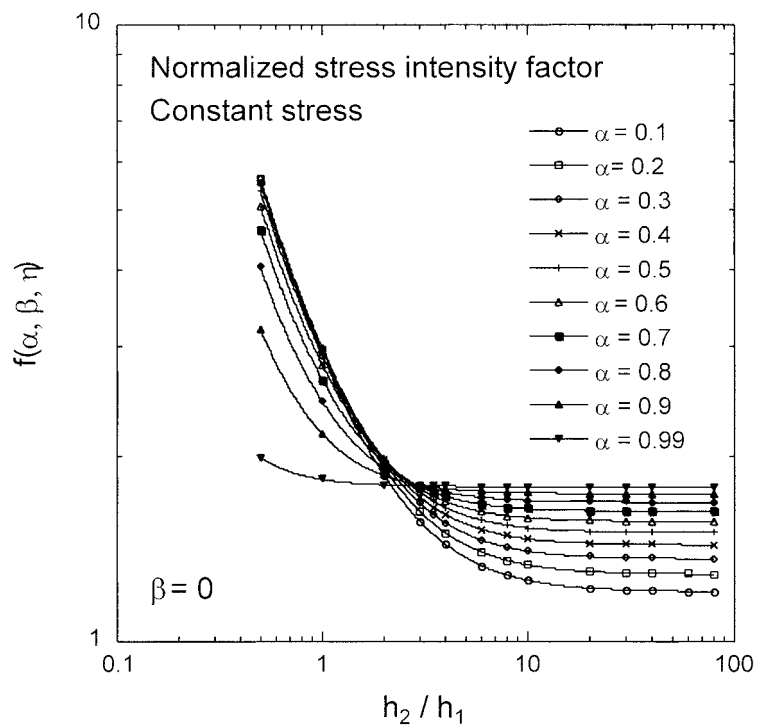


Figure 5. Normalized stress intensity factor as a function of substrate thickness for a film with a constant stress distribution. Substrate stiffer than film.

In the case of no elastic mismatch, s takes on the value of $1/2$ and Equation (9) reduces to the conventional definition for the stress intensity factor. The results of the numerical calculations are then presented by introducing a dimensionless stress intensity factor:

$$f(\alpha, \beta, \eta) = \frac{K_I}{\sigma_N(\pi h_1)^s}. \quad (10)$$

Here, σ_N is equal to $\bar{\sigma}$ for the constant stress distribution or to Δ for the case where the stress varies linearly. Since stress distributions are additive, the stress intensity factor for the general case where the stress varies as described by Equation (8), can be found by simply adding the appropriate stress intensity factors. Figures 4 and 5 show the dimensionless stress intensity factor as a function of substrate thickness for various degrees of elastic mismatch between film and substrate, assuming a constant stress distribution in the film. The stress intensity factor remains constant for thick substrates, but increases rapidly as the substrate thickness approaches that of the film. The results obtained for large substrate thicknesses are in excellent agreement with results obtained by Beuth (1991) for cracks in coatings on half spaces. The variation of $f(\alpha, \beta, \eta)$ with substrate thickness in the case of no elastic mismatch between film and substrate agrees with an equation reported by Tada et al. (1985). Figures 6 and 7 present the stress intensity factor as a function of α for $\beta = 0$ and $\beta = \alpha/4$, respectively. For an infinitely compliant substrate ($\alpha \rightarrow -1$), the stress intensity factor approaches zero, as expected. Similarly, the stress intensity factor converges to a value independent of substrate thickness for infinitely stiff substrates ($\alpha \rightarrow 1$). In between these two limiting cases, $f(\alpha, \beta, \eta)$ is very sensitive to substrate thickness. If the film is stiffer than the substrate ($\alpha < 0$), $f(\alpha, \beta, \eta)$ is virtually independent of the value of β ; if the substrate is stiffer ($\alpha > 0$), the effect of β is quite pronounced. Figures 8–11 depict numerical results for a film with a linear stress distribution. Since the stress in the film varies from $\Delta/2$ at the film surface to $-\Delta/2$ at the interface, the stress intensity factor can take on negative values. As long as the average stress $\bar{\sigma}$ in the coating is larger than $\Delta/2$ however, the total stress at the crack tip is tensile and the overall stress intensity factor is positive. As the thickness of the substrate decreases and substrate bending become more important, the stress intensity factor becomes positive and rises without bound. As before, the effect of β is most pronounced for positive values of α .

The change in elastic energy per unit crack length, ΔE , due to the introduction of the crack in a film is related to the steady-state energy release rate, G_{ss} , for a three-dimensional crack as it channels across the film (Figure 12) (Beuth, 1991). In the steady state, the energy released as the crack advances a distance da is given by $G_{ss}h_1 da$. This must be equal to the difference in potential energy between strips of width da upstream and downstream of the crack. Since the remote stress in the film does no work during cracking, this difference is equal to the strain energy difference between the strips. In other words, the steady-state energy release rate for a channeling crack must be equal to the change in elastic energy per unit crack length divided by h_1 :

$$G_{ss} = \frac{\Delta E}{h_1} = \frac{1}{2h_1} \int_0^{h_1} \sigma(y)\delta(y) dy. \quad (11)$$

Introducing Equation (8) for the stress distribution and applying the reciprocity principle lead to the following expression for the crack extension force:

$$G_{ss} = \frac{\pi \bar{\sigma}^2 h_1}{2 E_1} \left[g(\alpha, \beta, \eta) + 2 \left(\frac{\Delta}{\bar{\sigma}} \right) h(\alpha, \beta, \eta) + \left(\frac{\Delta}{\bar{\sigma}} \right)^2 k(\alpha, \beta, \eta) \right], \quad (12)$$

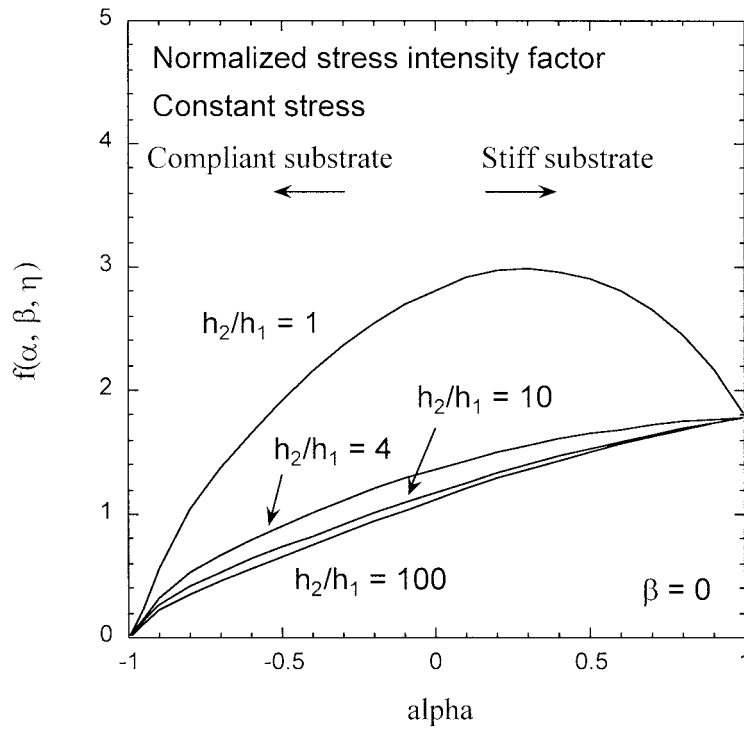


Figure 6. Normalized stress intensity factor as a function of α for a film with a constant stress distribution. The second Dundurs parameter, β , is taken to be zero.

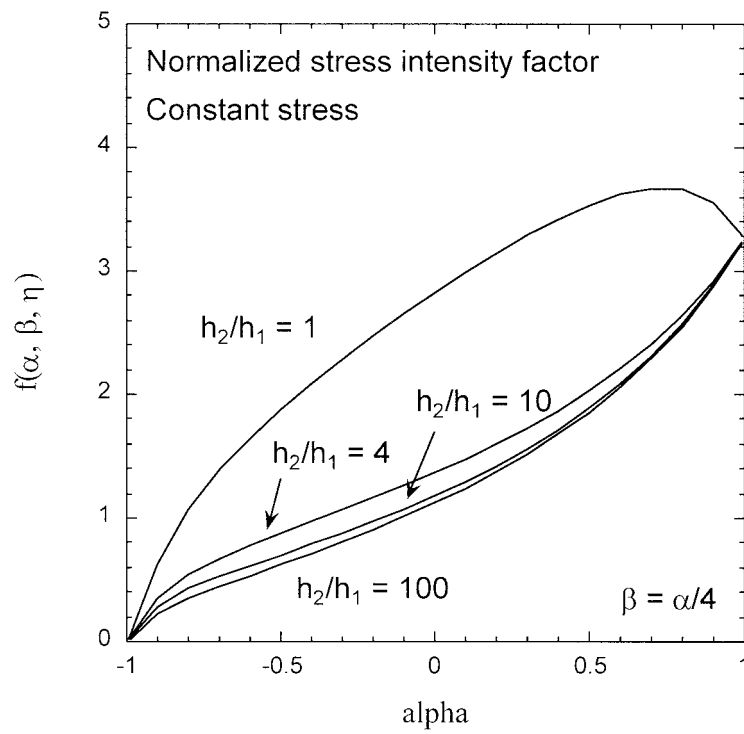


Figure 7. Normalized stress intensity factor as a function of α for a film with a constant stress distribution. The second Dundurs parameter, β , is taken to be $\alpha/4$.

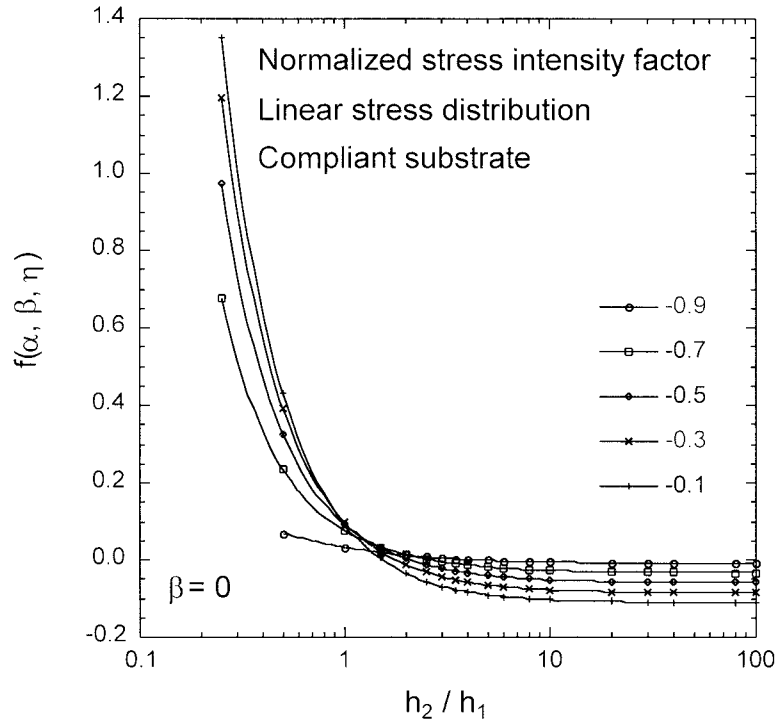


Figure 8. Normalized stress intensity factor as a function of substrate thickness for a film with a linear stress distribution. Substrate more compliant than film.

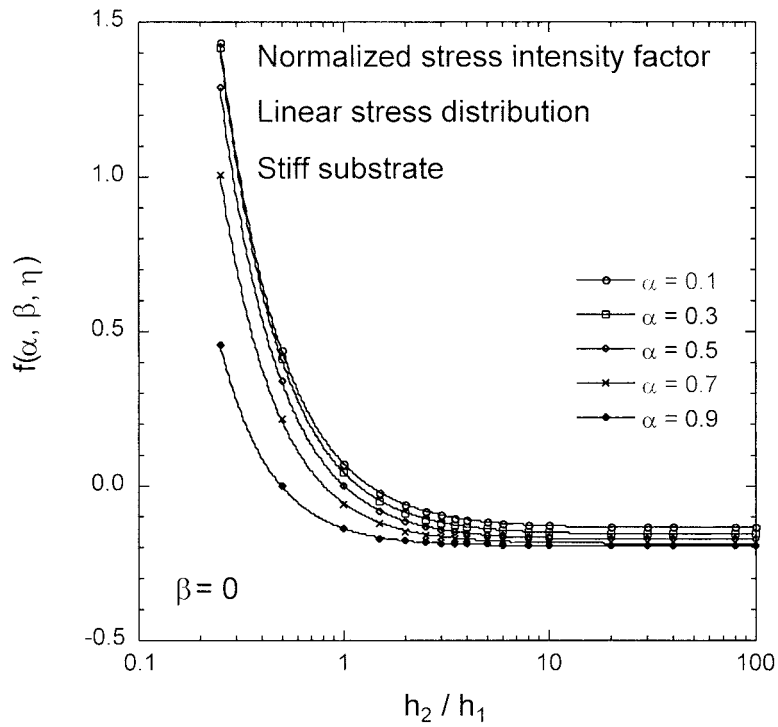


Figure 9. Normalized stress intensity factor as a function of substrate thickness for a film with a linear stress distribution. Substrate stiffer than film.

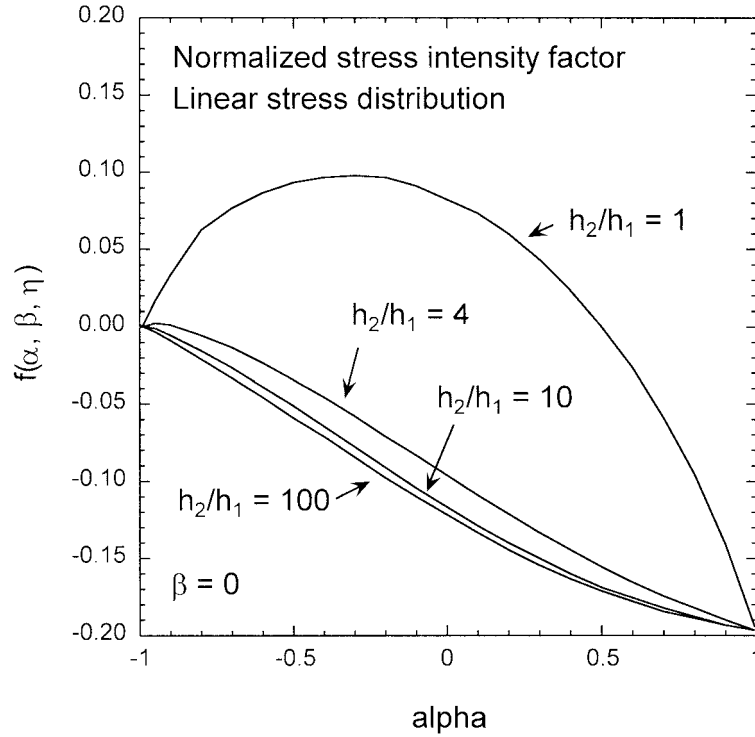


Figure 10. Normalized stress intensity factor as a function of α for a film with a linear stress distribution. The second Dundurs parameter, β , is taken to be zero.

where

$$g(\alpha, \beta, \eta) = \frac{\int_0^{h_1} \delta_{\bar{\sigma}}(y) dy}{\pi \frac{\bar{\sigma}}{E_1} h_1^2}, \quad (13)$$

$$h(\alpha, \beta, \eta) = \frac{\int_0^{h_1} \delta_{\Delta}(y) dy}{\pi \frac{\Delta}{E_1} h_1^2}, \quad (14)$$

$$k(\alpha, \beta, \eta) = \frac{\int_0^{h_1} \left(\frac{y}{h_1} - \frac{1}{2} \right) \delta_{\Delta}(y) dy}{\pi \frac{\Delta}{E_1} h_1^2}. \quad (15)$$

In these expressions, $\delta_{\bar{\sigma}}$ represents the crack opening displacement when the stress in the film is constant; δ_{Δ} is the displacement when the stress varies linearly. Thus, the functions $g(\alpha, \beta, \eta)$, and $h(\alpha, \beta, \eta)$ represent, respectively, the average crack opening displacements when the stress in the film is constant and when it varies linearly with film thickness. If the functions $g(\alpha, \beta, \eta)$, $h(\alpha, \beta, \eta)$, and $k(\alpha, \beta, \eta)$ are known, the crack extension force can

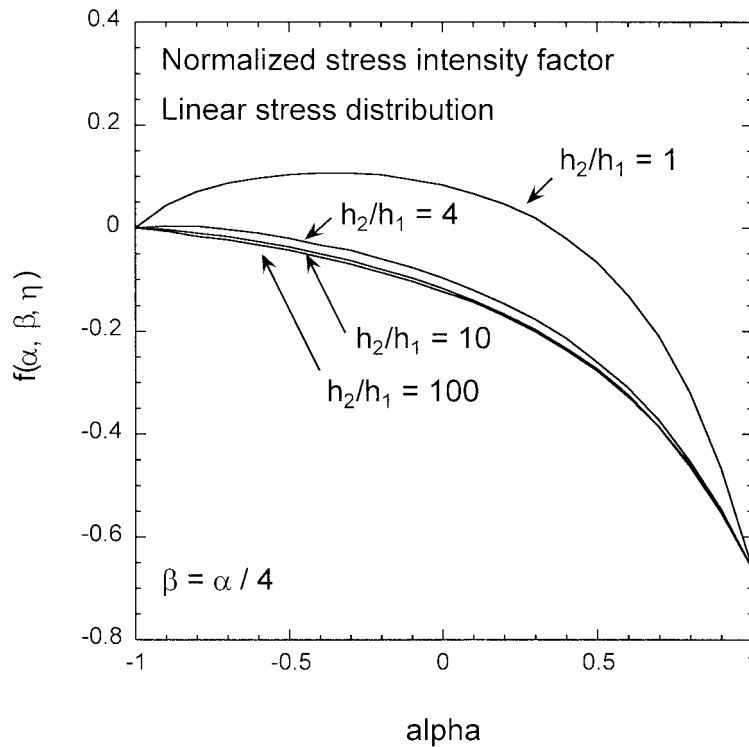


Figure 11. Normalized stress intensity factor as a function of α for a film with a linear stress distribution. The second Dundurs parameter, α , is taken to be $\alpha/4$.

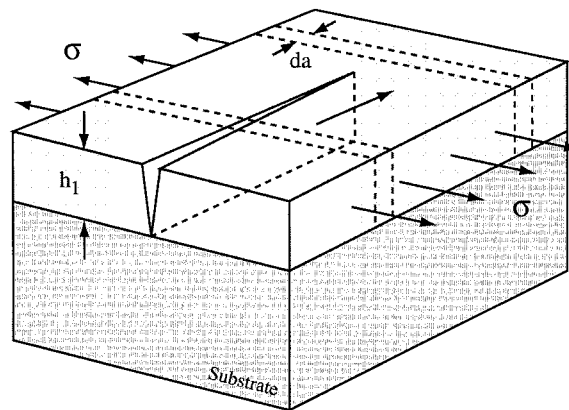


Figure 12. Channeling crack in a film with stress σ .

be calculated for arbitrary $\bar{\sigma}$ and Δ . Figures 13–22 present numerical data for these three functions. The results for $g(\alpha, \beta, \eta)$ and $h(\alpha, \beta, \eta)$ are qualitatively very similar. In both cases, the average crack opening displacement increases rapidly with decreasing substrate thickness, especially for compliant substrates (Figures 13, 14 and 17), although the displacement is larger for films with a constant stress distribution than for films in which the stress varies linearly. As expected, the crack opening displacement is independent of substrate thickness for infinitely stiff substrates ($\alpha \rightarrow 1$) and diverges for infinitely compliant substrates ($\alpha \rightarrow -1$) (Figures 15, 16, 18 and 19). The results show only a weak dependence on the

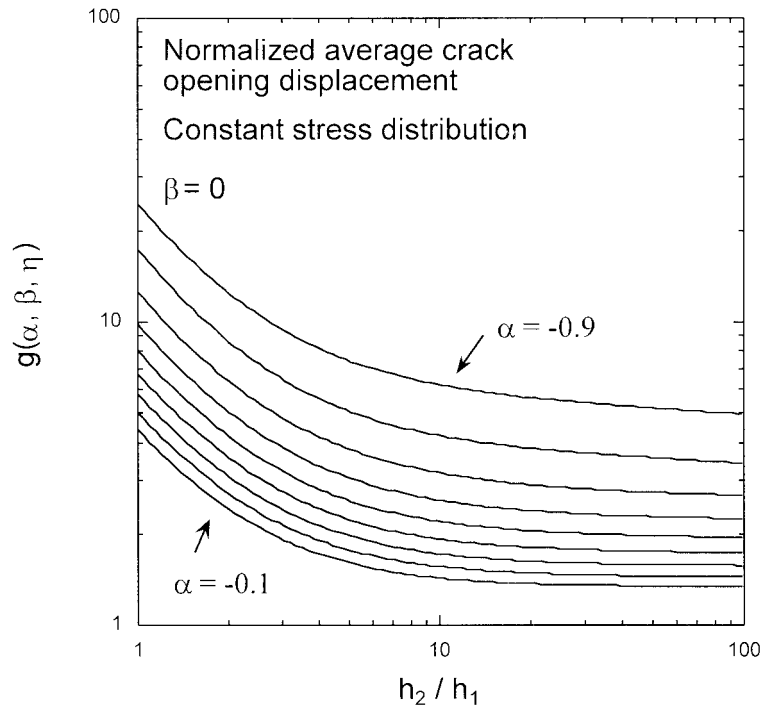


Figure 13. Normalized average crack opening displacement as a function of substrate thickness for a film with a constant stress distribution. Substrate more compliant than film. Results are shown for increments in α of 0.1.

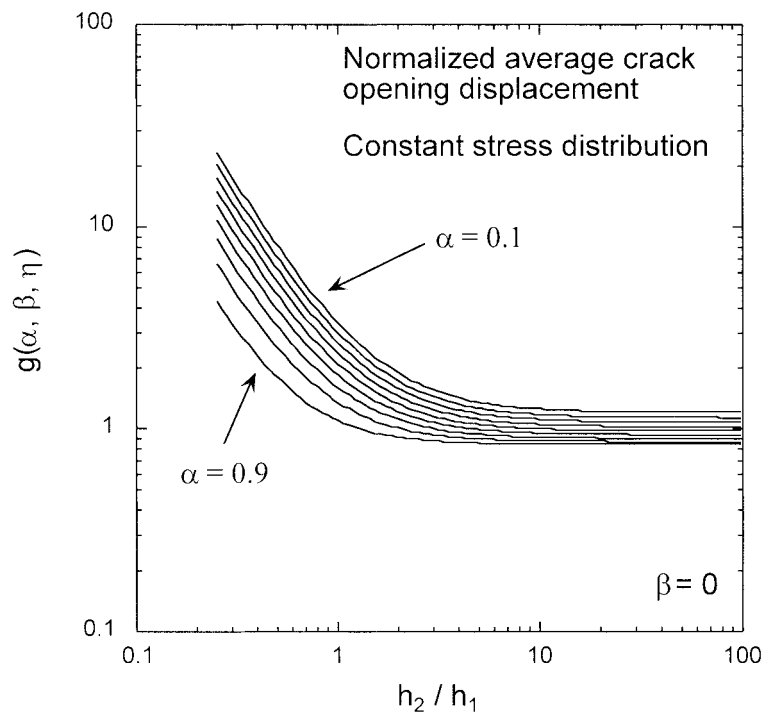


Figure 14. Normalized average crack opening displacement as a function of substrate thickness for a film with a constant stress distribution. Substrate stiffer than film. Results are shown for increments in α of 0.1.

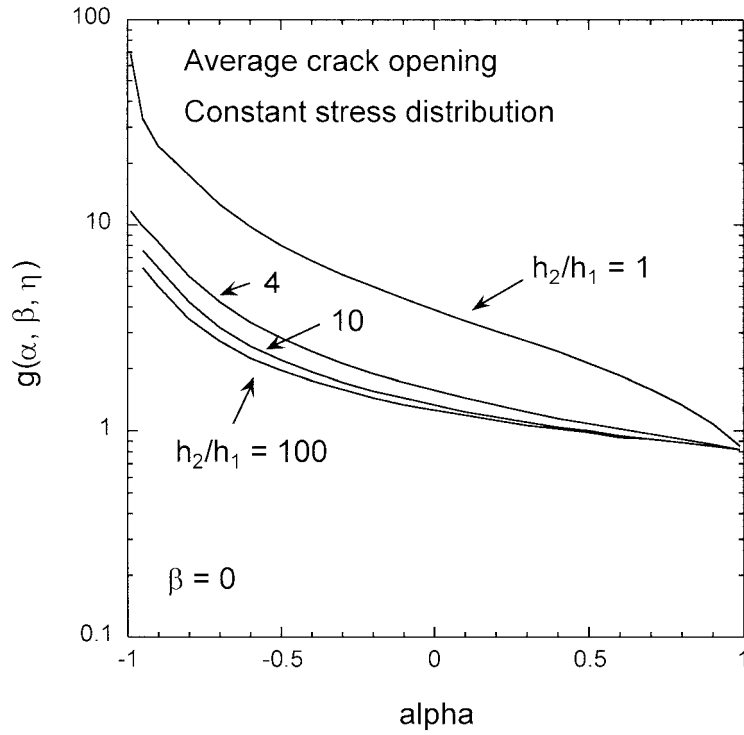


Figure 15. Normalized average crack opening displacement as a function of α for a film with a constant stress distribution. The second Dundurs parameter, β , is taken to be zero.

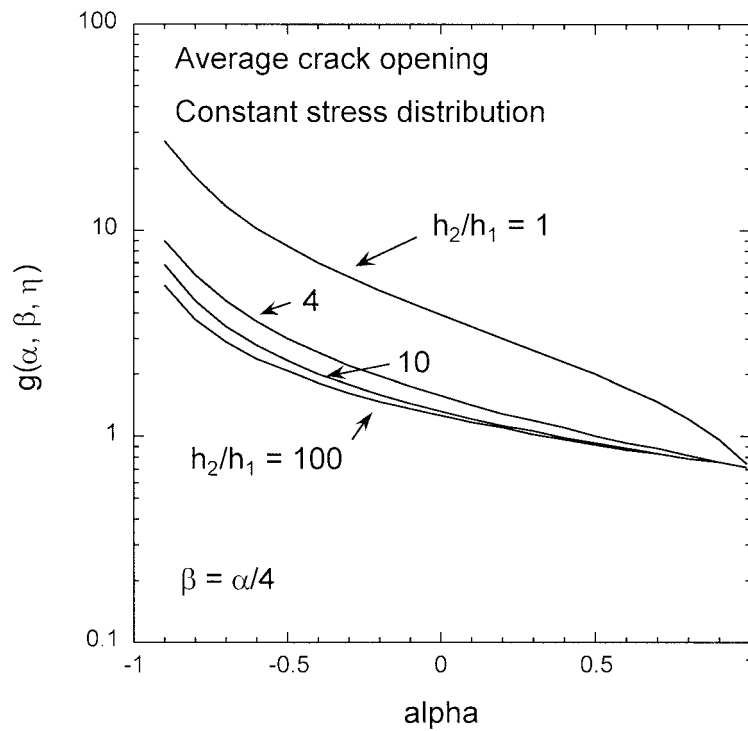


Figure 16. Normalized average crack opening displacement as a function of α for a film with a constant stress distribution. The second Dundurs parameter, β , is taken to be $\alpha/4$.

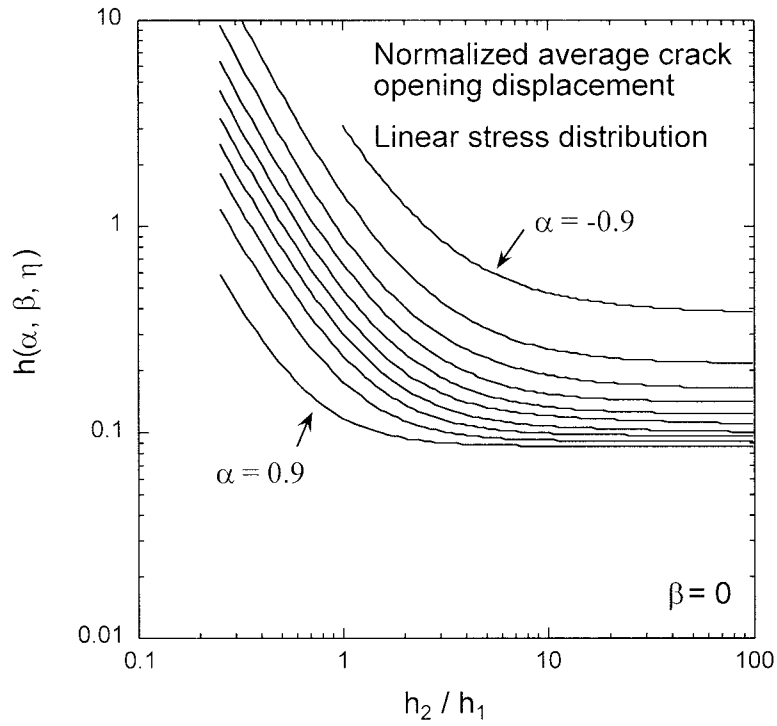


Figure 17. Normalized average crack opening displacement as a function of substrate thickness for a film with a linear stress distribution. Results are shown for increments in α of 0.2.

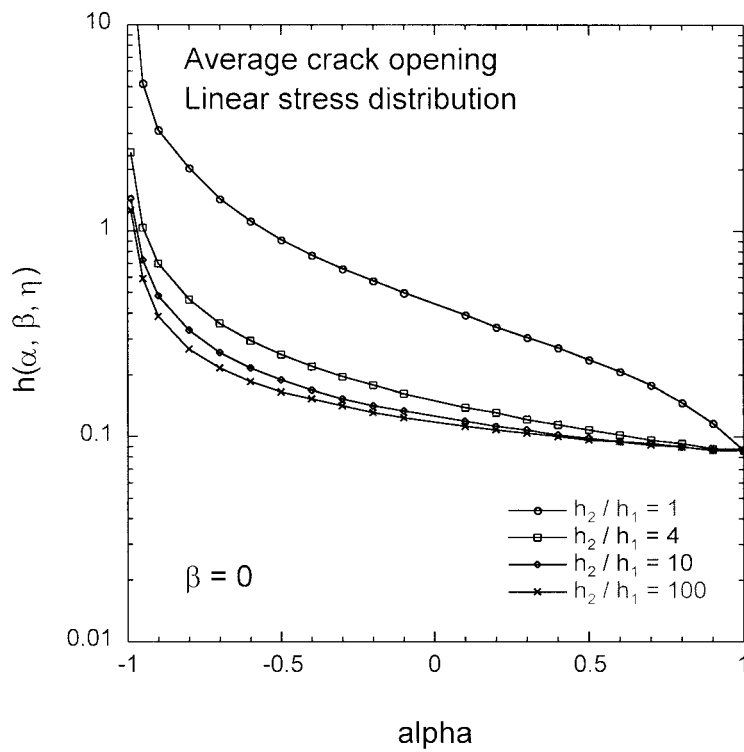


Figure 18. Normalized average crack opening displacement as a function of α for a film with a linear stress distribution. The second Dundurs parameter, β , is taken to be zero.

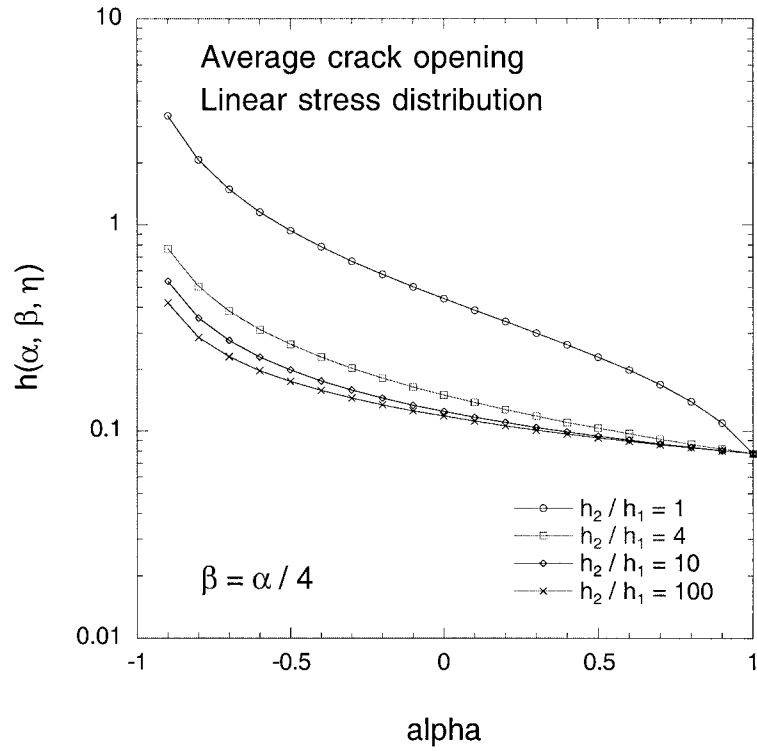


Figure 19. Normalized average crack opening displacement as a function of α for a film with a linear stress distribution. The second Dundurs parameter, β , is taken to be $\alpha/4$.

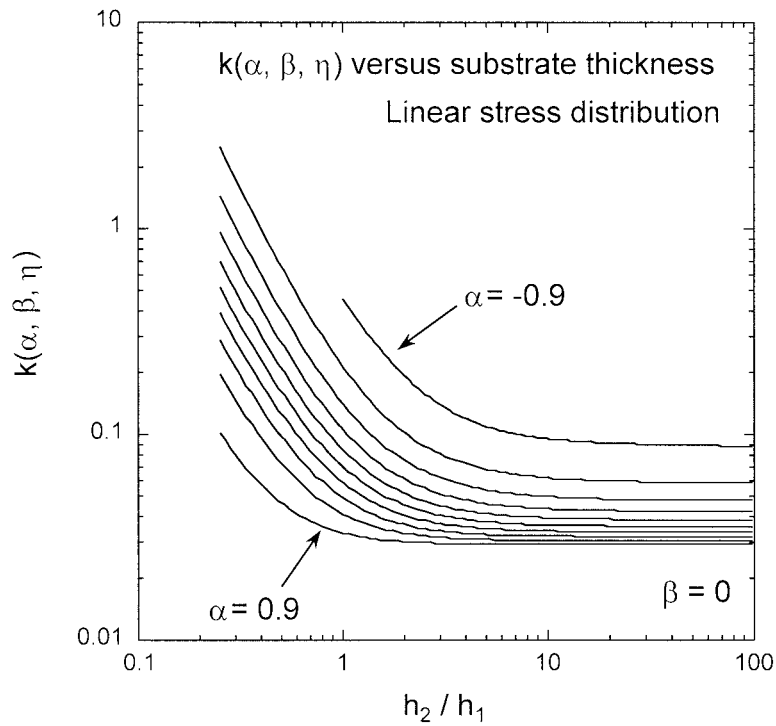


Figure 20. The function $k(\alpha, \beta, \eta)$ versus substrate thickness for a film with a linear stress distribution. Results are shown for increments in α of 0.2.

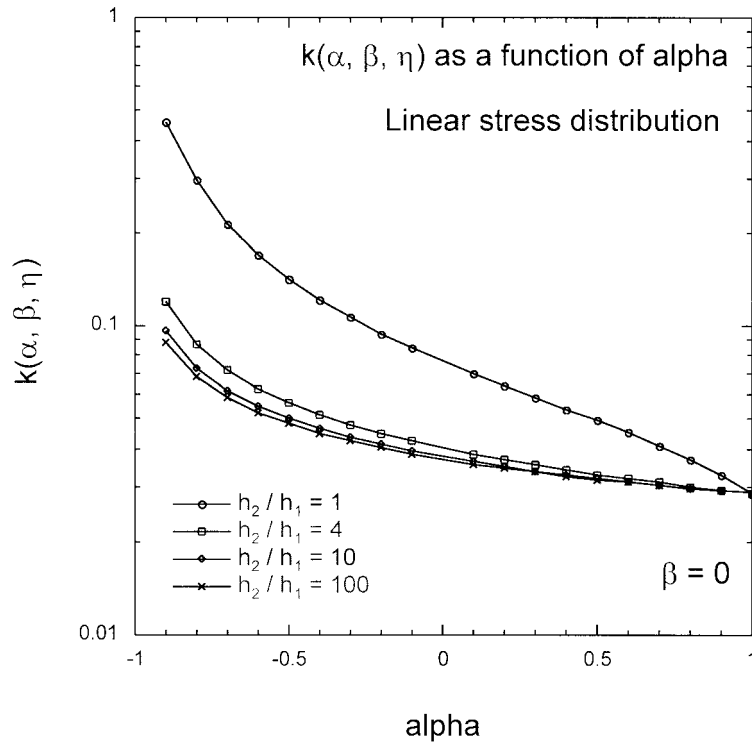


Figure 21. The function $k(\alpha, \beta, \eta)$ versus α for a film with a linear stress distribution. The second Dundurs parameter, β , is taken to be zero.

second Dundurs parameter β , although the dependence is somewhat stronger as α approaches unity. Figures 20–22 depict the results for the function $k(\alpha, \beta, \eta)$. The variation of $k(\alpha, \beta, \eta)$ with α , β and substrate thickness is similar to that of the other functions, although $k(\alpha, \beta, \eta)$ remains constant over a larger range of substrate thicknesses.

Figure 23 shows the steady state crack extension force calculated using Equation (12) for $\alpha = -0.9$. This elastic mismatch would be typical for a thin aluminum coating on a polyimide substrate. Two cases are considered: In the first case, the film is deposited with a constant residual stress and with the substrate clamped around its edge; in the second case the substrate is released after the deposition process and the stress in the film is allowed to relax by elastic deformation of the substrate. The substrate thickness has a substantial effect on crack extension force in both cases. If the substrate is clamped around the edge, a thinner substrate means that the residual stress in a larger part of the film is released as the channel crack propagates and the crack extension force increases with decreasing substrate thickness. If, however, the substrate is released, the residual stress in the coating is relaxed and the driving force for channel cracking is substantially reduced. This effect is important even for relatively thick substrates. Note that the contributions of $h(\alpha, \beta, \eta)$ and $k(\alpha, \beta, \eta)$ in Equation (12) are very small, except when the substrate thickness is comparable to the film thickness. The effect of substrate thickness on G_{ss} arises mainly from the thickness dependence of $g(\alpha, \beta, \eta)$ and $\bar{\sigma}$. Based on the results shown in Figure 23, one would expect a much larger driving force for channel cracking in a micromachined bilayer membrane than in a bilayer cantilever beam.

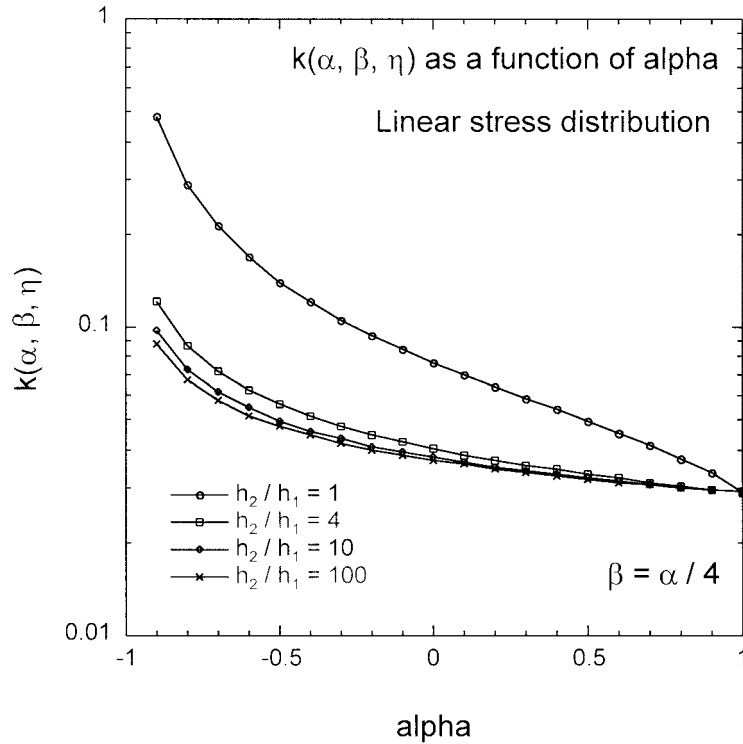


Figure 22. The function $k(\alpha, \beta, \eta)$ versus α for a film with a linear stress distribution. The second Dundurs parameter, β , is taken to be $\alpha/4$.

4. Applications

One application of the formulae derived in the previous sections is concerned with the change in curvature of a film/substrate assembly when channel cracking occurs in the film. Substrate curvature measurements are often used to determine the residual stress in a coating. The question then arises how film cracking affects the results obtained using this experimental technique. Consider a film on a compliant substrate with a stress distribution in the film described by Equation (8). The rotation of the ends of the substrate, $\Delta\vartheta$, due to the introduction of a single channel crack can be determined using the Reciprocal Theorem. The auxiliary problem consists of the same film/substrate assembly with the channel crack but with a bending moment per unit depth, $M^{(2)}$, applied to the edge of the substrate. This bending moment causes a crack opening displacement, $\delta^{(2)}(y)$. According to the Reciprocal Theorem, $\Delta\vartheta$ can be determined from

$$M^{(2)} \Delta\vartheta = \int_0^{h_1} \left[\bar{\sigma} + \left(\frac{y}{h_1} - \frac{1}{2} \right) \Delta \right] \delta^{(2)}(y) dy. \tag{16}$$

The crack opening displacement, $\delta^{(2)}(y)$, can be derived by realizing that the bending moment $M^{(2)}$ also generates a linear stress profile in the film:

$$\sigma^{(2)}(y) = \bar{\sigma}^{(2)} + \left(\frac{y}{h_1} - \frac{1}{2} \right) \Delta^{(2)}, \tag{17}$$

with

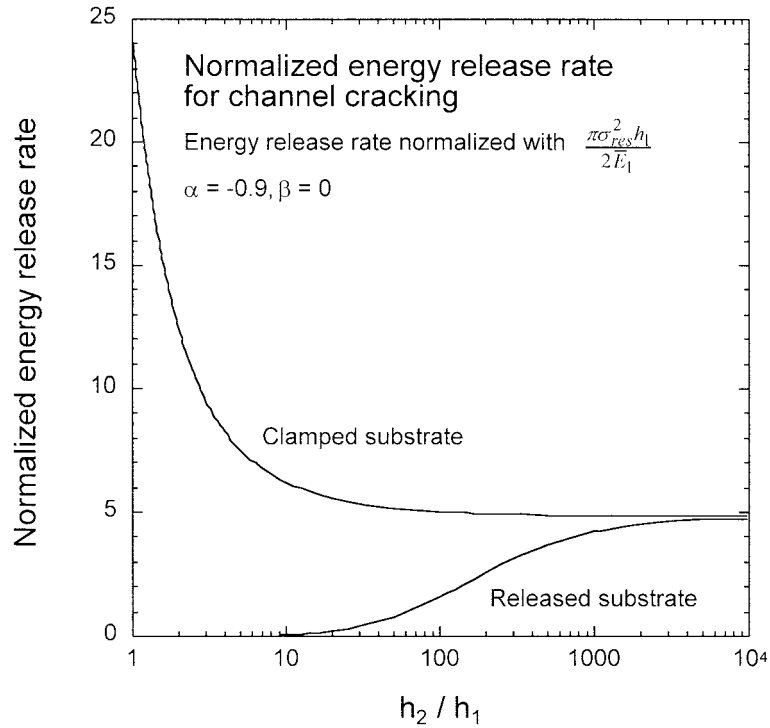


Figure 23. Normalized energy release rate for channel cracking in a film with a residual stress σ_{res} ; $\alpha = -0.9$, $\beta = 0$. The energy release rate is shown both for a clamped and a released substrate.

$$\bar{\sigma}^{(2)} = \frac{6(1 + \eta)\eta^2 \Xi}{(\Xi\eta^2 - 1)^2 + 4\Xi\eta(\eta + 1)^2} \frac{M^{(2)}}{h_1^2} = f_1(\eta, \Xi) \frac{M^{(2)}}{h_1^2},$$

$$\Delta^{(2)} = \frac{12(1 + \Xi\eta)\eta^3 \Xi}{(\Xi\eta^2 - 1)^2 + 4\Xi\eta(\eta + 1)^2} \frac{M^{(2)}}{h_1^2} = f_2(\eta, \Xi) \frac{M^{(2)}}{h_1^2},$$

and with $\Xi = \bar{E}_1/\bar{E}_2$. Thus, the method discussed in the previous section can be applied to determine $\delta^{(2)}(y)$. Taking into account the definitions in Equations (13)–(15), one finds after some algebra:

$$\Delta\vartheta = \frac{\pi\bar{\sigma}}{\bar{E}_1} \left[g(\alpha, \beta, \eta) f_1 + h(\alpha, \beta, \eta) f_2 + \left(\frac{\Delta}{\bar{\sigma}} \right) (l(\alpha, \beta, \eta) f_1 + k(\alpha, \beta, \eta) f_2) \right]. \quad (18)$$

Here, $l(\alpha, \beta, \eta)$ is defined as

$$l(\alpha, \beta, \eta) = \frac{\int_0^{h_1} \left(\frac{y}{h_1} - \frac{1}{2} \right) \delta_{\bar{\sigma}}(y) dy}{\pi \frac{\bar{\sigma}}{\bar{E}_1} h_1^2}. \quad (19)$$

Numerical results for $l(\alpha, \beta, \eta)$ are provided in Appendix 2. If multiple cracks form in the film, Equation (18) can be used to calculate the change in curvature of the substrate, provided the cracks are far enough apart to avoid interaction. Calculations by Thouless (1990) have shown that this is indeed the case if the crack spacing is greater than 8 film thicknesses, at

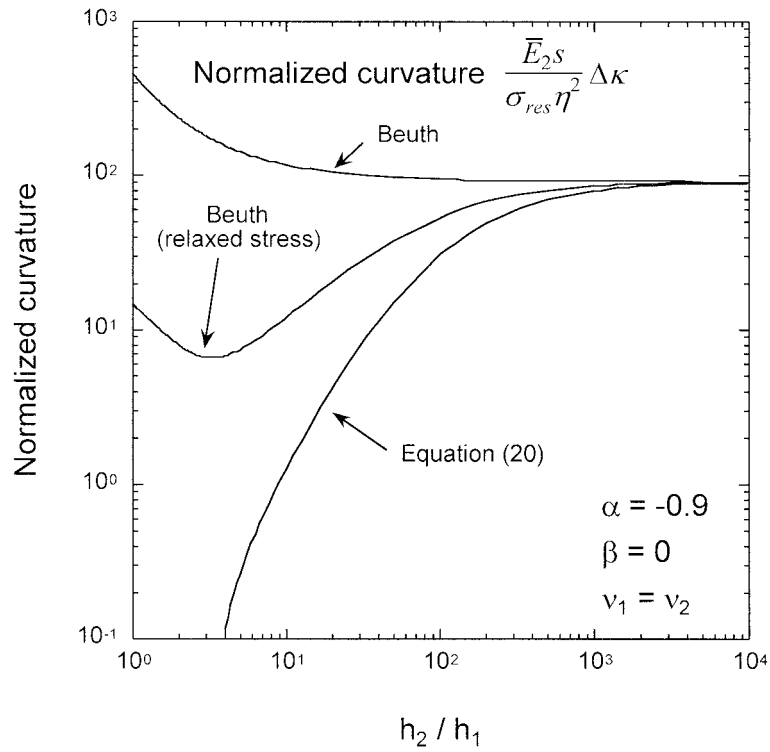


Figure 24. Change of substrate curvature induced by a channel crack in the film; $\alpha = -0.9$, $\beta = 0$.

least for systems with no elastic mismatch. If s is the average crack spacing, then the change of curvature of the substrate due to channel cracking is given by

$$\Delta\kappa = \frac{\pi\bar{\sigma}}{E_1s} \left[g(\alpha, \beta, \eta) f_1 + h(\alpha, \beta, \eta) f_2 + \left(\frac{\Delta}{\bar{\sigma}} \right) (l(\alpha, \beta, \eta) f_1 + k(\alpha, \beta, \eta) f_2) \right]. \quad (20)$$

If the substrate is much thicker than the film, this expression reduces to an equation derived by Beuth (1991) for the limiting case of a film on a half space. Figure 24 compares Equation (20) to Beuth’s equation for a substrate that is significantly more compliant than the film ($\alpha = -0.9$). Beuth’s equation is shown both for the case where the stress in the coating is σ_{res} and for the case where the stress is relaxed as described by Equation (8). Beuth’s equation greatly overestimates the change in curvature for substrates of finite thickness, although agreement between the two equations is better for stiffer substrates.

Another quantity of interest is the elastic extension of the substrate, Δ_s , when a channel crack forms in the film. This extension may be important for coated membranes, where cracking in the coating would relax the tension in the membrane and thus alter its mechanical characteristics. The approach to determining Δ_s is similar to that taken to calculate the change in curvature due to channel cracking and leads to the following expression:

$$\Delta_s = \frac{\pi\bar{\sigma}h_1}{E_1} \left[g(\alpha, \beta, \eta) f_3 + h(\alpha, \beta, \eta) f_4 + \left(\frac{\Delta}{\bar{\sigma}} \right) (l(\alpha, \beta, \eta) f_3 + k(\alpha, \beta, \eta) f_4) \right]. \quad (21)$$

Details of the derivation and the definitions of f_3 and f_4 can be found in Appendix 2. If the stress in the film is not allowed to relax, the substrate extension due to a channel crack is given by:

$$\Delta_s = \frac{\pi h_1^2 \sigma_{\text{res}}}{h_1 \bar{E}_1 + h_2 \bar{E}_2} g(\alpha, \beta, \eta). \quad (22)$$

Equation (21) reduces to Equation (22) when the substrate is significantly thicker than the film. For coated membranes, the thickness of the substrate layer may be comparable to that of the coating. Equation (21) predicts that in that case channel cracking has a significant impact on the overall compliance of a membrane.

5. Conclusions

Analysis of channel cracking in thin stressed films on compliant substrates shows that substrate thickness has a significant effect on the stress and displacement fields near a plane-strain crack. This is so for a wide range of elastic mismatch between film and substrate. Since the steady state crack extension force can be written in terms of normalized crack opening displacements, substrate thickness has a significant effect on the driving force for channel cracking. The boundary conditions for the substrate also play an important role: if the substrate is clamped around the edge, the initial residual stress in the coating cannot relax and as a result the crack extension force increases significantly with decreasing substrate thickness. If, on the other hand, the substrate is released, the stress in the coating relaxes and the driving force for cracking is reduced.

The results from this study can be applied directly to evaluate the change in curvature of the film/substrate assembly due to channel cracking, a quantity that may be of interest for the experimental determination of stresses in thin films. The extension of the substrate due to channel cracking can also be readily evaluated making it possible to determine the effect of cracking on the mechanical behavior of bilayer membranes. It is expected that the present study may lead to the development of new experimental techniques for measuring the fracture toughness of thin coatings by elastically straining both film and substrate.

Acknowledgements

The author gratefully acknowledges John Hutchinson for interesting discussions on the subject of channel cracking. This study was funded by the National Science Foundation CAREER Award DMR-0133559, the Harvard MRSEC DMR-98-09363, and by the Division of Engineering and Applied Sciences, Harvard University.

Appendix 1. The stress fields around an edge dislocation in a bilayer

The stress field around a dislocation in a bilayer can be found by decomposing the problem into two auxiliary problems: The problem of determining the stress field around a dislocation in an infinite bispaces, and the problem of determining the stress in a bilayer strip with prescribed tractions applied to its surfaces. The solution to the former (Figure 2b) can be found using complex potentials and is given by Suo (1989). The stress and displacement components can be written in terms of two complex potentials, $\Phi(z)$ and $\Omega(z)$:

$$\begin{aligned}
\sigma_{xx}^d + \sigma_{yy}^d &= 2[\Phi(z) + \overline{\Phi(z)}], \\
\sigma_{xx}^d + i\sigma_{xy}^d &= \overline{\Phi(z)} + \Omega(z) + (\bar{z} - z)\Phi'(z), \\
2\mu \frac{\partial}{\partial x}(u_x^d - u_y^d) &= \kappa \overline{\Phi(z)} - \Omega(z) - (\bar{z} - z)\Phi'(z),
\end{aligned} \tag{A1-1}$$

where $z = x + iy$. The analytic functions $\Phi(z)$ and $\Omega(z)$ are calculated from the potentials, $\Phi_0(z)$ and $\Omega_0(z)$, for an edge dislocation embedded in an infinite homogeneous material (Suo, 1989):

$$\Phi(z) = \begin{cases} \Phi_0(z) + \Pi \overline{\Omega_0(z)} \\ (1 + \Lambda)\Phi_0(z) \end{cases} \quad \text{and} \quad \Omega(z) = \begin{cases} \Omega_0(z) + \Lambda \overline{\Phi_0(z)} & z \text{ in 1,} \\ (1 + \Pi)\Omega_0(z) & z \text{ in 2.} \end{cases} \tag{A1-2}$$

Here, the constants Π and Λ are a measure for the inhomogeneity of the system and are defined as:

$$\Lambda = \frac{\alpha + \beta}{1 - \beta} \quad \text{and} \quad \Pi = \frac{\alpha - \beta}{1 + \beta}. \tag{A1-3}$$

The potentials $\Phi_0(z)$ and $\Omega_0(z)$, for an edge dislocation with unit Burgers vector parallel to the bimaterial interface and located at $(x = 0, y = \xi)$ are:

$$\Phi_0(z) = \frac{-iE_1}{8\pi(1 - \nu_1^2)} \frac{1}{z - i\xi} \quad \text{and} \quad \Omega_0(z) = \frac{iE_1}{8\pi(1 - \nu_1^2)} \left[\frac{2i\xi}{(z - i\xi)^2} + \frac{1}{z - i\xi} \right]. \tag{A1-4}$$

Analytical expressions of the stress components due to a dislocation in an infinite bimaterial can be readily derived from Equations (A1-1) through (A1-4).

The problem of determining the stresses in a bilayer strip with prescribed tractions (Figure 2c) is solved using Fourier transforms with two real potentials $U(x, y)$ and $\chi(x, y)$ (Civelek, 1985; Suo and Hutchinson, 1989) that satisfy

$$\Delta^2 U = 0, \quad \Delta \chi = 0, \quad \frac{\partial^2 \chi}{\partial x \partial y} = \frac{1}{4} \Delta U, \tag{A1-5}$$

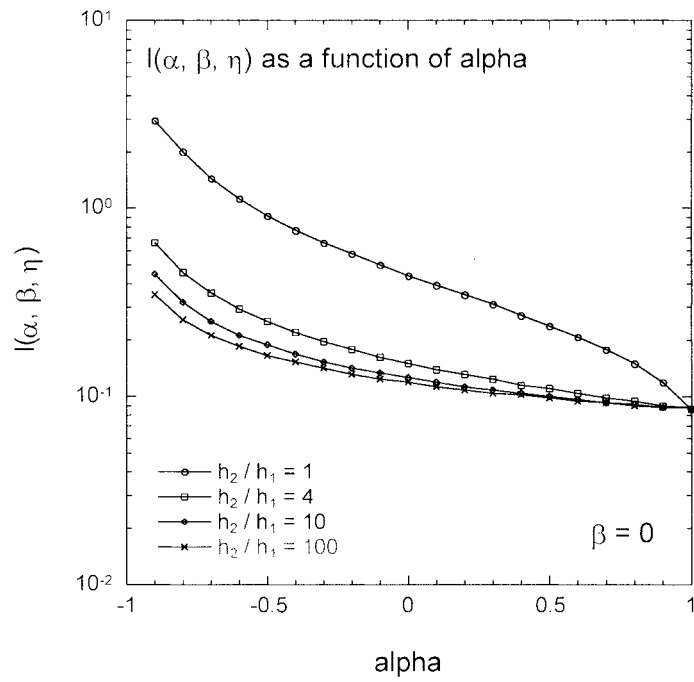
where $\Delta = \partial^2/\partial x^2 + \partial^2/\partial y^2$. The stress and displacement components in the bimaterial strip can be determined from

$$\begin{aligned}
\sigma_{xx}^s &= \frac{\partial^2 U}{\partial y^2}, \quad \sigma_{yy}^s = \frac{\partial^2 U}{\partial x^2}, \quad \sigma_{xy}^s = -\frac{\partial^2 U}{\partial x \partial y}, \\
2\mu u_x^s &= -\frac{\partial U}{\partial x} + (\kappa + 1) \frac{\partial \chi}{\partial y}, \quad 2\mu u_y^s = -\frac{\partial U}{\partial y} + (\kappa + 1) \frac{\partial \chi}{\partial x}.
\end{aligned} \tag{A1-6}$$

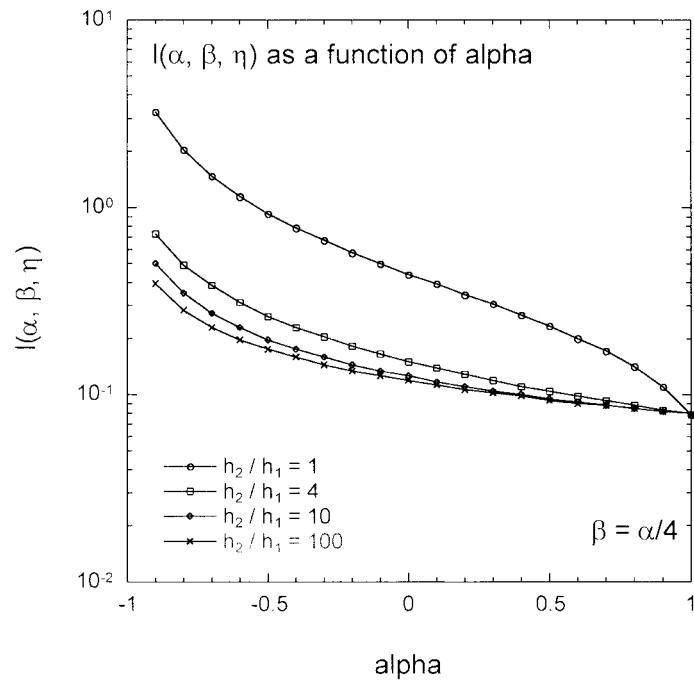
For each layer, the functions $U(x, y)$ and $\chi(x, y)$ can be represented by Fourier integrals:

$$\begin{aligned}
U(x, y) &= \int_0^\infty \left\{ \left[\frac{A_1}{\lambda^2} + \frac{A_2}{\lambda} y \right] e^{-\lambda y} + \left[\frac{A_3}{\lambda^2} + \frac{A_4}{\lambda} y \right] e^{\lambda y} \right\} \cos \lambda x \, d\lambda, \\
\chi(x, y) &= \int_0^\infty \frac{1}{2\lambda^2} \{ A_2 e^{-\lambda y} + A_4 e^{\lambda y} \} \sin \lambda x \, d\lambda.
\end{aligned} \tag{A1-7}$$

Since there are two layers, a total of eight constants A_i need to be determined. The A_i are found by matching the tractions and displacements along the interface and by satisfying the boundary conditions at the top and bottom surfaces of the bilayer strip. In order to do so, the



(a)



(b)

Figure A1. The function $l(\alpha, \beta, \eta)$ versus α ; (a) $\beta = 0$, (b) $\beta = \alpha/4$.

Fourier transforms of the tractions applied to these surfaces need to be calculated. After the A_i have been determined, the stress and displacement components in the bimaterial strip can be derived in a straightforward manner, although the Fourier integrals need to be evaluated numerically.

Appendix 2. Substrate extension due to channel cracking

Consider a film on a compliant substrate with a film stress distribution described by Equation (8). The auxiliary problem consists of the of the same substrate with the channel crack but with a normal force per unit depth, $N^{(3)}$, applied to the edge of the substrate. This force causes a crack opening displacement, $\delta^{(3)}(y)$. According to the Reciprocal Theorem, Δ_s is given by

$$N^{(3)}\Delta_s = \int_0^{h_1} \left[\bar{\sigma} + \left(\frac{y}{h_1} - \frac{1}{2} \right) \Delta \right] \delta^{(3)}(y) dy. \quad (\text{A2-1})$$

The crack opening displacement, $\delta^{(3)}(y)$, can be derived by realizing that the normal force, $N^{(3)}$, also generates a linear stress profile in the film:

$$\sigma^{(3)}(y) = \bar{\sigma}^{(3)} + \left(\frac{y}{h_1} - \frac{1}{2} \right) \Delta^{(3)} \quad (\text{A2-2})$$

with

$$\bar{\sigma}^{(3)} = \frac{\Xi\eta(1 + 3\eta + 3\eta^2 + \eta^3\Xi)}{(\Xi\eta^2 - 1)^2 + 4\Xi\eta(\eta + 1)^2} \frac{N^{(3)}}{h_1} = f_3(\eta, \Xi) \frac{N^{(3)}}{h_1},$$

$$\Delta^{(3)} = \frac{-6(\Xi - 1)\eta^3\Xi}{(\Xi\eta^2 - 1)^2 + 4\Xi\eta(\eta + 1)^2} \frac{N^{(3)}}{h_1} = f_4(\eta, \Xi) \frac{N^{(3)}}{h_1}.$$

Thus, the method discussed in the previous sections can be applied to determine $\delta^{(3)}(y)$. Taking into account the definitions in Equations (13), (14), (15) and (19), one finds after some algebra:

$$\Delta_s = \frac{\pi\bar{\sigma}h_1}{E_1} \left[g(\alpha, \beta, \eta) f_3 + h(\alpha, \beta, \eta) f_4 + \left(\frac{\Delta}{\bar{\sigma}} \right) (l(\alpha, \beta, \eta) f_3 + k(\alpha, \beta, \eta) f_4) \right]. \quad (\text{A2-3})$$

For completeness, Figure A1 depicts $l(\alpha, \beta, \eta)$ as a function of α and β . From the figure it is apparent that the effect of changes in β is minimal. If multiple cracks occur in the film, Equation (A2-3) can be used to calculate the strain of the substrate, E_s , provided the cracks are far enough apart to avoid interaction:

$$E_s = \frac{\pi\bar{\sigma}h_1}{E_1s} \left[g(\alpha, \beta, \eta) f_3 + h(\alpha, \beta, \eta) f_4 + \left(\frac{\Delta}{\bar{\sigma}} \right) (l(\alpha, \beta, \eta) f_3 + k(\alpha, \beta, \eta) f_4) \right]. \quad (\text{A2-4})$$

References

- Beuth, J.L., Jr. (1991). Cracking of thin bonded films in residual tension. *International Journal of Solids and Structures* **29**, 1657–1675.
- Civelek, M.B. (1985). *Stress Intensity Factors for a System of Cracks in an Infinite Strip*. vol. STP 868: ASTM.

- Cook, R.F. and Liniger, E.G. (1999). Stress-corrosion cracking of low-dielectric-constant spin-on-glass thin films. *Journal of the Electrochemical Society* **146**, 4439–4448.
- Dundurs, J. (1969). Edge-bonded dissimilar orthogonal wedges. *Journal of Applied Mechanics* **36**, 650–652.
- Gecit, M.R. (1979). Fracture of a surface layer bonded to a half space. *International Journal of Engineering Science* **17**, 287–295.
- Hutchinson, J.W. and Suo, Z. (1991). Mixed mode cracking in layered materials. *Advances in Applied Mechanics* **29**, 63–191.
- Lu, M.-C. and Erdogan, F. (1983a). Stress intensity factors in two bonded elastic layers containing cracks perpendicular to and on the interface-I. Analysis. *Engineering Fracture Mechanics* **18**, 491–506.
- Lu, M.-C. and Erdogan, F. (1983b). Stress intensity factors in two bonded elastic layers containing cracks perpendicular to and on the interface-II. Solution and results. *Engineering Fracture Mechanics* **18**, 507–528.
- Press, W.H., Teukolsky, S.A., Vetterling, W.T. and Flannery, B.P. (1996). *Numerical Recipes in Fortran 77*, 2nd ed. Cambridge University Press, Cambridge.
- Suga, T., Elssner, E. and Schmander, S. (1988). Composite parameters and mechanical compatibility of material joints. *Journal of Composite Materials* **22**, 917–934.
- Suo, Z. (1989). Singularities interacting with interfaces and cracks. *International Journal of Solids and Structures* **25**, 1989.
- Suo, Z. and Hutchinson, J.W. (1989). Steady-state cracking in brittle substrates beneath adherent films. *International Journal of Solids and Structures* **25**, 1337–1353.
- Suo, Z. and Hutchinson, J.W. (1990). Interface crack between two elastic layers. *International Journal of Fracture* **43**, 1–18.
- Tada, H., Paris, P.C. and Irwin, G.R. (1985). *The Stress Analysis of Cracks Handbook*. Paris Productions Inc., St. Louis.
- Thouless, M.D. (1990). Crack spacing in brittle films on elastic substrates. *Journal of the American Ceramic Society* **73**, 2144–2146.
- Zak, A.R. and Williams, M.L. (1963). Crack point singularities at a bimaterial interface. *Journal of Applied Mechanics* **30**, 142–143.